

1 **Increasing knock-in efficiency in mouse zygotes by transient hypothermia**

2 Amine Bouchareb<sup>1</sup>, Daniel Biggs<sup>1</sup>, Samy Alghadban<sup>1</sup>, Christopher Preece<sup>1</sup>, Benjamin Davies<sup>1,2,\*</sup>

3 <sup>1</sup>Wellcome Centre for Human Genetics, Oxford, UK, OX3 7BN

4 <sup>2</sup>The Francis Crick Institute, London, UK, NW1 1AT

5 \*Corresponding author

6

7 Short running title: Cold shock increases knock-in efficiency in mouse zygotes

8 Key words: Gene editing, zygote, electroporation, homology directed repair.

9

10 **Abstract**

11 Integration of a point mutation to correct or edit a gene requires the repair of the CRISPR-Cas9-induced  
12 double-strand break by homology directed repair (HDR). This repair pathway is more active in late S and  
13 G2 phases of the cell cycle, whereas the competing pathway of non-homologous end joining (NHEJ)  
14 operates throughout the cell cycle. Accordingly, modulation of the cell cycle by chemical perturbation or  
15 simply by the timing of gene editing to shift the editing towards the S/G2 phase has been shown to  
16 increase HDR rates.

17 Using a traffic light reporter in mouse embryonic stem cells and a fluorescence conversion reporter in  
18 human induced pluripotent stem cells, we confirm that a transient cold shock leads to an increase in the  
19 rate of HDR, with a corresponding decrease in the rate of NHEJ repair. We then investigated whether a  
20 similar cold shock could lead to an increase in the rate of HDR in the mouse embryo.

21 By analysing the efficiency of gene editing using SNP changes and loxP insertion at 3 different genetic  
22 loci, we found that a transient reduction in temperature after zygote electroporation of CRISPR-Cas9  
23 ribonucleoprotein with an ssODN repair template did indeed increase knock-in efficiency, without  
24 affecting embryonic development. The efficiency of gene editing with and without the cold shock was  
25 first assessed by genotyping blastocysts. As a proof of concept, we then confirmed that the modified  
26 embryo culture conditions were compatible with live births by targeting the coat colour gene Tyrosinase  
27 and observing the repair of the albino mutation. Taken together, our data suggest that a transient cold  
28 shock could offer a simple and robust way to improve knock-in outcomes in both stem cells and zygotes.

29

## 30 **Introduction**

31 Genetically altered animal models provide invaluable insights into human biology, disease pathology,  
32 and allow therapeutic approaches to be tested and optimized. In the mouse, targeted gene  
33 manipulation has been routine for several decades, originally achieved using homologous recombination  
34 in embryonic stem (ES) cells to remove or replace sequences <sup>1</sup>. More recently, the emergence of site-  
35 specific DNA endonucleases such as Zinc Finger Nucleases (ZFN) <sup>2</sup>, Transcription Activator-Like Effector  
36 Nucleases (TALENs) <sup>3</sup> and the CRISPR-Cas RNA-dependent nucleases <sup>4-6</sup>, has increased the efficiency of  
37 targeted manipulation, allowing direct manipulation of the zygote.

38 The CRISPR-Cas9 system, in particular, has become the technology of choice for genetic alteration due  
39 to its simplicity of design <sup>7</sup>. However, one of the challenges of using nucleases for the generation of  
40 targeted replacement or knock-in mutations are the competing repair mechanisms that operate to  
41 process the nuclease-induced double strand break. The repair pathways most active in the mammalian  
42 cell are non-homologous end joining (NHEJ) and microhomology-mediated end joining (MMEJ) which  
43 lead to insertion and deletion (indel) mutations at the target site. Although highly useful for achieving  
44 knock-out mutations by ablating gene sequences and shifting open-reading frames, the significant repair  
45 pathways used to achieve targeted gene replacements using co-introduced homology repair templates,  
46 for example homology directed repair (HDR), operate at considerably lower efficiencies <sup>8</sup>. Subsequently,  
47 following the introduction of CRISPR-Cas9 into mouse zygotes with a suitable repair template designed  
48 to achieve a targeted knock-in, most embryos undergo indel mutagenesis (via non-homology end joining  
49 (NHEJ) or microhomology-mediated end joining (MMEJ)) rather than targeted repair using the  
50 introduced template (via HDR mechanisms).

51 To overcome this challenge, researchers are exploring strategies to alter the balance in repair outcomes  
52 in favour of achieving the desired knock-in event. The delivery route used to deliver CRISPR-Cas9

53 reagents and donor template to zygotes or cells<sup>9,10</sup>, the choice of the Cas nuclease<sup>11,12</sup> and the format  
54 of the repair template<sup>13-16</sup> can be optimized to significantly improve knock-in efficiency. In addition,  
55 chemical modification of the DNA repair pathways by inhibiting key components of the NHEJ and/or  
56 MMEJ pathways or promoting aspects of the HDR pathway have been shown to improve knock-in  
57 outcome in cells<sup>17-19</sup> and embryos<sup>20-22</sup>.

58 The timing of the delivery of the Cas9 ribonucleoprotein (RNP) complex and HDR template with respect  
59 to the cell cycle has also been explored. Whilst NHEJ is active throughout the cell cycle, the HDR repair  
60 mechanism is more active during the S and G2 cell cycle phases<sup>23,24</sup>. Thus, manipulating cell cycle  
61 progression by prolonging the S/G2 phases can help improve knock-in outcomes<sup>25,26</sup>. Indeed, the long  
62 G2 phase in the 2-cell mouse embryo has been exploited to increase knock-in efficiency by introducing  
63 the gene editing reagents at this developmental stage<sup>27</sup>.

64 The use of cell cycle or DNA repair pathway inhibitors on embryos might have a negative impact on  
65 embryonic development or may have other non-specific effects such as increased levels of off-target  
66 mutations. An alternative strategy reported in cells, involves no chemical intervention and is simply to  
67 induce a cold shock by reducing the temperature for a short period of time. It has been reported that  
68 this manipulation resulted in the accumulation of nucleases proteins and enhanced the mutagenesis  
69 efficiency for both ZFNs and TALENs in cells<sup>28,29</sup>. Several recent studies have reported an improvement  
70 in the HDR rates using CRISPR-Cas9 in human induced pluripotent stem (iPS) cells<sup>30-32</sup>. The use of  
71 CRISPR-Cas9 in combination with a cold shock has not been thoroughly investigated *in vivo*. However,  
72 Remy et al., showed a beneficial effect of a short mild hypothermic treatment on HDR-mediated  
73 transgene integration in rat zygotes injected with TALENs<sup>33</sup>. Although no significant changes in targeting  
74 efficiency were reported in this study, the authors concluded that the increased trend in targeting  
75 efficiency warranted further examination. It seems likely that the cold shock could be exerting its effect

76 through alterations to the cell cycle, but the mechanisms involved in this stimulation of gene knock-in  
77 efficiency remain unclear.

78 In this study, we have investigated the application of cold-shock on the efficiency of knock-in alleles  
79 when CRISPR-Cas9 machinery is introduced into the mouse zygote, exploring 3 independent gene loci.  
80 We first verified the effects of moderate transient hypothermia on repair outcomes in human iPS cells  
81 and mouse ES cells using fluorescent reporters. We then explored whether this manipulation can be  
82 applied in the mouse zygote and here report conditions that lead to a stimulation of knock-in efficiency.  
83 We demonstrate by the production of live mice that the conditions are compatible with normal  
84 subsequent mouse development.

## 85 **Materials and methods**

### 86 Cell lines and cell culture

87 Human iPS cells (KOLF2-C1) were cultured in Essential 8™ (E8) medium (STEMCELL Technologies,  
88 #A1517001) on tissue culture flasks coated with Vitronectin diluted per manufacturer's instructions  
89 (Gibco™ #A14700) and with daily medium changes. For passaging, the cells were washed with PBS and  
90 treated with TrypLE™ Select (Thermo Scientific™, #12563011) or using ReLeSR™ (STEMCELL  
91 Technologies, #05872) for 5 min and cell pellets re-plated at the required density in Essential 8™ (E8)  
92 medium supplemented with 5 μM Y-27632 (Rock Inhibitor, Sigma-Aldrich).

93 Mouse JM8F6 ES cells were cultured in Knockout DMEM (LifeTechnologies) supplemented with 2 mM L-  
94 Glutamine, 1× non-essential amino acids, 0.1 mM β-mercaptoethanol, 1000 U/ml ESGRO (Millipore) and  
95 10% fetal bovine serum (LifeTechnologies) on tissue culture flasks on a feeder layer of mouse embryonic  
96 fibroblasts or on plates coated with 0.1% Gelatin after electroporation. For routine passage of stem cells  
97 grown on feeders, confluent flasks were washed twice with pre-warmed PBS and trypsinized with

98 Trypsin (0.5% Trypsin, 0.1% chicken serum, 20 µg/ml EDTA, 10 µg/ml D-Glucose in PBS) for 8 minutes at  
99 37°C then replated at the required density in medium.

#### 100 iPS cell fluorescent reporter system

101 A KOLF2-C1 human iPS cell line with a single copy of a CAGGS promoter-driven GFP cassette within the  
102 *AAVS1* safe harbour locus was generated via Bxb1 recombinase mediated cassette exchange. A generic  
103 *AAVS1* targeting vector (Addgene #22075) was adapted by replacing the SA-T2A-Puromycin resistance  
104 cassette with a CAGGS promoter driving a Hygromycin-P2A-Bxb1 integrase cDNA cassette with Bxb1 attP  
105 sites flanking the open reading frame. Following gene targeting in KOLF2-C1 cells, recombinant iPS cells  
106 were transfected with a shuttle vector containing Bxb1 attB sites flanking a loxP-flanked promoterless  
107 Neomycin cassette followed by a promoterless GFP open reading frame. Expression of the Bxb1  
108 integrase from the *AAVS1* targeted docking site catalysed the cassette exchange, resulting in neomycin  
109 resistant iPS cells with a GFP cassette integrated. The GFP cassette was then activated by transient  
110 expression of Cre recombinase (Supplementary Figure 1A), delivered by lipofection of a pCre-Pac vector  
111 <sup>34</sup>.

#### 112 ES cell traffic light reporter system

113 A JM8F6 mouse ES cell line with a single copy of a CAGGS promoter-driven inactive mRFP1 cassette  
114 (with a STOP codon at amino-acid position 30, followed by a 27 bp deletion encompassing amino acid  
115 positions 33-41), followed by an out-of-frame P2A-eGFP cassette and a rabbit beta globin  
116 polyadenylation sequence was targeted to the *Gt(ROSA26)Sor* locus by gene targeting. A targeting  
117 vector for the *Gt(ROSA26)Sor* locus, pROSA26.10 (hygro attP) was obtained as a kind gift from Ralf  
118 Kuehn <sup>35</sup> which contained homology arms, a diphtheria toxin A chain (dtA) negative selection cassette  
119 and a PGK driven hygromycin resistance cassette. The dtA cassette and a portion of the 3' homology  
120 arm was excised, creating a shortened targeting vector. A CAGGS promoter-driven inactive mRFP1

121 cassette (with the aforementioned mutations), followed by an out-of-frame P2A-GFP cassette was  
122 generated by gene synthesis and cloned between the two homology arms). Gene targeting was  
123 performed using standard conditions and recombinant clones were screened for targeted integration as  
124 previously described <sup>36</sup>.

#### 125 CRISPR Reagents and delivery

126 CRISPR guide RNAs were designed using the CRISPOR algorithm (<http://crispor.tefor.net>). The guide  
127 sequences were ordered from Synthego as chemically modified single guide-RNAs (sgRNA). Alt-R<sup>®</sup> S.p.  
128 HiFi Cas9 Nuclease V3 was obtained from IDT. The HDR templates were designed as 135 nt single-  
129 stranded oligodeoxynucleotides (ssODN) with homology arms flanking sequences on both sides of the  
130 cut-site. Silent mutations were introduced within the PAM sites to prevent recutting. For the ssODN  
131 designs used for the in-vivo study, an extra silent mutation was introduced within the guide RNA  
132 recognition sequence to create a diagnosis restriction site to simplify genotyping.

133 Cas9 protein (890 nM) / sgRNA (1.48 μM) were delivered as ribonucleoprotein complexes with ssODN  
134 (3.7 μM) to 1x10<sup>5</sup> cells (human iPS or mouse ES) using the ThermoFisher Neon Electroporation System  
135 (10 μl) (1200V, 30ms, 2 pulses). Immediately following the electroporation, the cells were either  
136 incubated at 30°C for 24h followed by 48h at 37°C or were incubated at 37°C for 72h in a 5% CO<sub>2</sub>  
137 incubator. At 72h post-electroporation, cells were detached using Trypsin (ES) or TrypLE™ Select (iPS)  
138 and analyzed with a BD LSRFortessa™ X-20 Cell Analyzer (BD Biosciences).

139 Sequences of the sgRNA, ssODN donors and the genotyping primers used in the study are listed in  
140 Supplementary Tables 1 and 2.

#### 141 Zygote electroporation

142 3-week old wild-type C57BL/6J or albino B6(Cg)-Tyr<sup>c-2l</sup> /J female mice (Charles River) were superovulated  
143 and mated with wild-type or albino C57BL/6J studs. Fertilized oocytes were prepared from plugged  
144 females and up to 100 embryos were electroporated in Opti-MEM media (ThermoFisher Scientific)  
145 containing 130 ng/μl sgRNA and 650 ng/ul Cas9 protein (Alt-R® S.p. HiFi Cas9 Nuclease V3, IDT). ssODN  
146 templates for homology directed repair were added to the electroporation mix at a final concentration  
147 of 430 ng/μl. Electroporation was performed with the previously described conditions<sup>9</sup>. The  
148 electroporation was performed between 22 and 24 h after the hCG injection. Electroporated zygotes  
149 were either cultured overnight at 37°C or immediately cultured for 6 hours at 30°C followed by 37°C to  
150 the two-cell stage in EmbryoMax Advanced KSOM (Merck) and surgically implanted into recipient  
151 pseudopregnant CD1 females, or were cultured in vitro in KSOM-AA medium until blastocyst stage.

#### 152 Genomic DNA extraction and PCR amplification of edited regions

153 In vitro cultured blastocysts were lysed using standard conditions and crude lysate DNA was used to  
154 amplify the region of interest. The target gene was amplified using the primers listed in Supplementary  
155 Table 1. PCR products were denatured, reannealed and analysed on a 15% polyacrylamide gel to detect  
156 the formation of heteroduplexes indicative of mutations, as previously described<sup>9</sup>. Restriction  
157 endonuclease digestion was used to determine successful homology directed repair and digested PCR  
158 product were analysed on a 2% agarose gel, followed by confirmatory Sanger sequencing.

#### 159 Animal work

160 All animal studies received ethical approval from the Clinical Medicine AWERB (Animal Welfare and  
161 Ethical Review Body) at the University of Oxford and were performed in accordance with UK Home  
162 Office Animals (Scientific Procedures) Act 1986 under project license PAA2AAE49. Mice were housed in  
163 individually ventilated cages and received food and water ad libitum. All surgery was performed under  
164 isoflurane inhalation anaesthesia using appropriate pre-surgical analgesia.

165 Statistical analysis

166 Comparison of the knock-in efficiency for the different culture conditions in stem cells was performed  
167 using the t-test. The efficiencies of editing and HDR for the embryo study were tested using a logistic  
168 regression model. Each result was assigned a set of indicator variables to label which experimental  
169 method was used and which target gene was addressed. The experimental conditions (control or cold  
170 shock conditions) were treated as fixed-effects and the genes as random-effects. The model was then fit  
171 using the function `glmmer` (family = binomial) from the R package `lme4`. The blastocyst development  
172 comparison was performed using a two-sided Fisher's exact test. Data sets were analysed and presented  
173 using Graphpad Prism software v8.4.

## 174 **Results**

### 175 **Cold shock stimulates HDR in human iPS cells**

176 We first wanted to confirm previous reports which showed the potential benefit of a transient cold  
177 shock on the rate of HDR in cells<sup>30-32</sup> in two independent cell types of different species. We designed  
178 two different strategies, both relying on fluorescence indicators to signal either the HDR or the NHEJ  
179 events to confirm this phenomenon in mouse embryonic stem (ES) cells and human induced pluripotent  
180 stem (iPS) cells.

181 In human iPS cells, a single copy of GFP under the control of a CAGGS promoter was integrated at the  
182 *AAVS1* locus and stable uniform fluorescence was confirmed (Supplementary Figure 1A). A gene editing  
183 strategy was adopted which aimed to convert the GFP into BFP via the incorporation of a Y66H  
184 mutation. Successful HDR would thus generate blue fluorescence, whereas disruptive indel mutations  
185 caused by NHEJ would abolish fluorescence (Figure 1A).



186 In order to assess the efficiency of HDR after a cold shock treatment, we electroporated the cells with  
187 Cas9/sgRNA (Supplementary Table 1) with the required ssODN (Supplementary Table 2) and cultured  
188 them, either at 37°C for 72h (control group) or 30°C for 24h then 37°C for 48h (cold shock group). Flow  
189 cytometry was used to evaluate the proportion of human iPS cells that express GFP or BFP or where  
190 fluorescence had been extinguished.

191 Cells incubated at 30°C for 24h showed a significantly higher GFP to BFP conversion than cells cultured  
192 without the cold shock ( $P=0.0252$ ), suggesting a higher HDR repair frequency. Furthermore, the  
193 proportion of non-fluorescent cells due to inactivation of the GFP cassette by NHEJ-induced indel  
194 mutations was significantly higher in the cells cultured under normal condition ( $P=0.0052$ ) than those  
195 receiving the cold shock (Figure 1B). The cold shock yielded an 28% increase in HDR efficiency (Figure  
196 1C) and the HDR/NHEJ ratio was increased by 1.7-fold when compared to the control group (Figure 1D).

#### 197 **Cold shock stimulates HDR in mouse ES cells**

198 To investigate the effect of the cold shock in a different cell line, we designed a Traffic Light Reporter  
199 system<sup>37</sup> using a CAGGS driven mRFP1 cassette fused to a GFP cassette via a P2A sequence to allow  
200 bicistronic expression of the two fluorophores. The mRFP1 sequence was rendered non-functional by  
201 deleting 27 bp and additional mutations were included to ensure the downstream P2A-GFP sequence  
202 was out-of-frame. This construct was integrated at the *Gt(ROSA)26Sor* safe harbour locus of mouse ES  
203 cells (JM8F6) via gene targeting. A sgRNA was designed to target the mutated sequence of mRFP1  
204 (Supplementary Table 1) and an 150 nt ssODN was designed to repair the deletion to restore the mRFP1  
205 expression (Supplementary figure 1B, Supplementary Table 2). Using this strategy, mRFP1 will only  
206 result if a successful repair event has occurred via HDR, with no expression of GFP occurring due to an  
207 inframe stop codon at the end of the mRFP1 cassette. In contrast, if the repair event proceeds via NHEJ

208 and an indel mutation is incorporated, no mRFP1 fluorescence will result but a +2 frame-shift mutation  
209 would restore the expression of the downstream GFP (Figure 2A).

210 In order to assess the efficiency of HDR after a cold shock treatment, we electroporated the cells with  
211 RNP with the required ssODN and cultured them, either at 37°C for 72h (control group) or 30°C for 24h  
212 then 37°C for 48h (Cold Shock Group). Flow cytometry was used to evaluate the proportion of mouse ES  
213 cells that express GFP and mRFP1.

214 Although, the overall editing efficiency in mouse ES cells was quite low, we observed a significant 2-fold  
215 increase in HDR efficiency for the cells that were incubated at 30°C, compared to the control cells  
216 ( $P=0.0006$ ; Figure 2C). The NHEJ (using the GFP signal as a proxy) was significantly reduced by 1.2-fold  
217 for the cold shock group ( $P=0.003$ ; Figure 2C). Moreover, their ratio of HDR/NHEJ was 2.4-fold higher  
218 when compared to the group of cells that were cultured under normal conditions ( $P=0.0003$ ; Figure 2D).

219 Taking together these results confirm previously reported data on the effect of cold shock in improving  
220 precise gene repair by favouring HDR pathways over NHEJ and shows the phenomenon to be consistent  
221 in mouse stem cells.

## 222 **Cold shock stimulates HDR in mouse zygotes**

223 Having confirmed that cold shock leads to an increase in the efficiency of knock-in allele production in  
224 mouse and human stem cells, we explored whether the effects of cold shock on HDR rate could be  
225 replicated *in vivo* by modifying the culture conditions of the mouse zygote following delivery of CRISPR-  
226 Cas9.

227 Firstly, different incubation times at 30°C were tested on cultured embryos to establish whether  
228 incubation at this unconventional temperature resulted in normal development and survival rates.

229 Incubation of mouse embryos at 30°C for 24 hours post-harvest, did indeed result in a very low survival

230 rate with very few embryos progressing to the 2-cell stage (data not shown). Restricting this lower  
231 temperature to a period of between 6-8 hours post-harvest resulted in normal 2-cell progression  
232 (Supplementary Figure 2A;  $P=0.058$ ) and further embryo culture tests showed that the rate of blastocyst  
233 development was also unaffected by this duration of 30°C incubation (Supplementary Figure 2B;  
234  $P=0.786$ ). Further investigations revealed no difference between 6 and 8 hours of 30°C incubation (6  
235 hours – 9.4% HDR; 8 hours – 10% HDR), therefore, we decided to limit the length of time the embryos  
236 were incubated at 30°C to 6h followed by a return to the conventional 37°C until they reached the  
237 blastocyst stage (Figure 3A).

238 Having established a cold shock regime which was compatible with mouse preimplantation  
239 development, we tested the effect on gene editing outcomes using sgRNAs addressing three  
240 independent gene loci (*Kcnab1*, *Tyr* and *Jcad*) (Supplementary Table 1) together with ssODNs to  
241 introduce mutations into these loci (Supplementary table 2). Embryos were cultured to the blastocyst  
242 stage, lysed and analysed for mutagenesis via PAGE electrophoresis and DNA sequencing  
243 (Supplementary Table 3). Culturing the embryos under cold shock conditions showed a significant  
244 improvement in HDR rate across the sgRNAs tested ( $\beta=0.985$ ,  $P=0.005$ ), when analysed on a gene basis  
245 (Figure 3B) or on a session basis (Figure 3C) with an average increase of in HDR efficiency of 1.9-fold  
246 compared to normal culture conditions. Notably, the overall editing (including both Indel and knock-in  
247 mutations) was not impacted by the culture conditions ( $\beta=0.417$ ,  $P=0.491$ , Figure 3D).

#### 248 **Production of live pups following the cold shock embryo culture conditions**

249 Having shown a positive impact of the 6 hours cold-shock on editing efficiencies in cultured mouse  
250 embryos, in order to confirm that the cold-shock procedure did not interfere with subsequent in vivo  
251 development, we conducted a proof-of-concept in vivo study, using the Tyrosinase sgRNA and an ssODN  
252 to correct the R77L mutation responsible for the albino phenotype in B6(Cg)-*Tyr*<sup>c-2j</sup> /J mice

253 (Supplementary Table 1 & 2). After electroporation, embryos were cultured under normal conditions or  
254 cold shock conditions, then transferred to pseudo-pregnant females. Live pups were born from both  
255 groups, indicating that the cold-shock treatment did not adversely affect mouse development  
256 (Supplementary table 4). Furthermore, the litter size obtained in our study was comparable between  
257 groups. Although not of sufficient scale to allow a statistical analysis of the cold shock effect for live pup  
258 production, it was notable that in the litters born from the cold shock treated embryos, two entirely  
259 black pups were obtained, whereas in the litters born from the control cultured embryos, only a single  
260 mosaic pigmented pup was obtained (Figure 3E).

261 In summary, the results of our study confirm that the cold-shock induced augmentation of HDR  
262 efficiencies is common to both mouse and human stem cells and also preimplantation mouse embryos  
263 and the cold-shock procedure is compatible with the production of gene edited mouse models.

## 264 **Discussion**

265 In this study, we investigated the impact of modifying the culture temperature on DNA repair pathway  
266 for Cas9-induced double strand breaks in both human and mouse stem cells and the mouse zygote.  
267 Although a number of chemical modifications have been shown to enhance HDR rate, application of  
268 such approaches to the mouse zygote may not be the preferred approach due to negative impacts on  
269 early embryonic development. Thus, a simple intervention which requires no chemical or small molecule  
270 additions to the embryo culture media was sought. Here, we wanted to test the hypothesis that, similar  
271 to the effects of transient cold shock demonstrated in cultured cells<sup>30-32</sup>, such an intervention could also  
272 promote higher levels of HDR in the mouse zygote.

273 Studies in human iPS cells have shown that cell cycle and gene expression are affected by moderate  
274 hypothermia. Maurissen et al. found that cold shock had various effects in human iPS cells: it slowed  
275 cell-cycle progression, resulting in an accumulation of cells in G2/M phase, reduced DNA synthesis rate

276 and enhanced the frequency of homology-directed repair<sup>32</sup>. Exposure of iPS cells to 32°C for 24 or 48  
277 hours led to a 2-fold increase in the rate of HDR<sup>31</sup>. When combined with small molecule enhancer of  
278 HDR and stabilizing chemical modification of the ssODN template, an additive effect was observed  
279 favouring the HDR pathway and resulting in a seven-fold higher ratio of HDR to NHEJ<sup>30</sup>.

280 Our results also confirm that culturing human iPS cells under cold-shock conditions (30°C for 24h)  
281 improves the efficiency of knock-in and reduces the rate of NHEJ-induced indel mutations, resulting in a  
282 1.7-fold higher ratio HDR to NHEJ when compared to control conditions at 37°C. Similarly, when similar  
283 culture conditions were tested on mouse ES cells, we found that repair bias also shifted toward HDR  
284 over NHEJ, leading to 2.4-fold higher HDR/NHEJ ratio.

285 This same stimulation of HDR/NHEJ was seen in our in vivo experiments with the delivery of CRISPR-Cas9  
286 and ssODN reagents by electroporation. It would be interesting to explore whether the transient  
287 hypothermic culture conditions slows the cell cycle progression or alters the duration of the S/G2 phase,  
288 potentially providing an explanation of why the lower temperature culture also stimulates the HDR  
289 repair, as previously shown in iPS cells<sup>32</sup>.

290 Previous work with Zinc Finger nucleases and TALENs has explored the effects of transient hypothermia  
291 on mutagenesis rates in general. A study with zinc finger nucleases reported higher levels of  
292 mutagenesis and proposed a mechanism of reduced protein turnover of the nuclease at colder  
293 temperatures.<sup>28</sup> A similar effect of cold-shock was found for mutagenesis levels induced by TALENs.  
294 Editing rates at the *HBG1* and *HBG2* loci increased ~2-fold when human CD34<sup>+</sup> peripheral blood stem  
295 cells were exposed to 30°C cold shock for 16 hours compared with 37°C culture<sup>38</sup>. In contrast, we saw  
296 no overall increase in editing efficiency in our zygote and stem cell studies, with the cold-shock  
297 specifically affecting the relative proportion of repair via HDR.

298 Despite the interest that researchers have shown in the study of cold shock impact on gene editing  
299 outcomes in vitro using multiple cell lines, the impact of such conditions in vivo have remained poorly  
300 investigated. In summary, we have confirmed that a 6-hour cold-shock increases the efficiency of  
301 targeted mutagenesis when CRISPR-Cas9 reagents and template are delivered to the mouse zygote,  
302 whilst not impacting overall mouse development. Using this simple intervention to improve knock-in  
303 efficiencies could help reduce the animal cost of genetically altered knock-in mouse production.

#### 304 **Funding statement**

305 This work was supported by the Wellcome Trust (Core Award Grant, 203141/Z/16/Z) and by a  
306 National Centre for the Replacement, Refinement and Reduction of Animals in Research grant  
307 (NC/R001014/1).

#### 308 **Author confirmation/contribution statement**

309 A.B., D.B, S.A. and C.P. performed the mouse mutagenesis, the animal husbandry and molecular biology.  
310 A.B. and B.D. analysed the data and wrote the paper, with input from all authors.

#### 311 **Authors disclosure**

312 The authors declare no competing interests

#### 313 **References**

- 314 1. Capecchi MR. Gene targeting in mice: functional analysis of the mammalian genome for the  
315 twenty-first century. *Nature reviews Genetics* 2005;6(6):507-12, doi:10.1038/nrg1619
- 316 2. Bibikova M, Carroll D, Segal DJ, et al. Stimulation of homologous recombination through  
317 targeted cleavage by chimeric nucleases. *Molecular and cellular biology* 2001;21(1):289-97,  
318 doi:10.1128/mcb.21.1.289-297.2001
- 319 3. Mussolino C, Alzubi J, Fine EJ, et al. TALENs facilitate targeted genome editing in human cells  
320 with high specificity and low cytotoxicity. *Nucleic acids research* 2014;42(10):6762-73,  
321 doi:10.1093/nar/gku305
- 322 4. Mali P, Yang L, Esvelt KM, et al. RNA-guided human genome engineering via Cas9. *Science (New*  
323 *York, NY)* 2013;339(6121):823-6, doi:10.1126/science.1232033

- 324 5. Cong L, Ran FA, Cox D, et al. Multiplex genome engineering using CRISPR/Cas systems. *Science*  
325 (New York, NY) 2013;339(6121):819-23, doi:10.1126/science.1231143
- 326 6. Jinek M, East A, Cheng A, et al. RNA-programmed genome editing in human cells. *eLife*  
327 2013;2(e00471, doi:10.7554/eLife.00471
- 328 7. Jinek M, Chylinski K, Fonfara I, et al. A programmable dual-RNA-guided DNA endonuclease in  
329 adaptive bacterial immunity. *Science* (New York, NY) 2012;337(6096):816-21,  
330 doi:10.1126/science.1225829
- 331 8. Xue C, Greene EC. DNA Repair Pathway Choices in CRISPR-Cas9-Mediated Genome Editing.  
332 *Trends in genetics : TIG* 2021;37(7):639-656, doi:10.1016/j.tig.2021.02.008
- 333 9. Alghadban S, Bouchareb A, Hinch R, et al. Electroporation and genetic supply of Cas9 increase  
334 the generation efficiency of CRISPR/Cas9 knock-in alleles in C57BL/6J mouse zygotes. *Scientific reports*  
335 2020;10(1):17912, doi:10.1038/s41598-020-74960-7
- 336 10. Xu X, Gao D, Wang P, et al. Efficient homology-directed gene editing by CRISPR/Cas9 in human  
337 stem and primary cells using tube electroporation. *Scientific reports* 2018;8(1):11649,  
338 doi:10.1038/s41598-018-30227-w
- 339 11. Howden SE, McColl B, Glaser A, et al. A Cas9 Variant for Efficient Generation of Indel-Free  
340 Knockin or Gene-Corrected Human Pluripotent Stem Cells. *Stem cell reports* 2016;7(3):508-517,  
341 doi:10.1016/j.stemcr.2016.07.001
- 342 12. Idoko-Akoh A, Taylor L, Sang HM, et al. High fidelity CRISPR/Cas9 increases precise monoallelic  
343 and biallelic editing events in primordial germ cells. *Scientific reports* 2018;8(1):15126,  
344 doi:10.1038/s41598-018-33244-x
- 345 13. Iyer S, Mir A, Vega-Badillo J, et al. Efficient Homology-Directed Repair with Circular Single-  
346 Stranded DNA Donors. *The CRISPR journal* 2022;5(5):685-701, doi:10.1089/crispr.2022.0058
- 347 14. Richardson CD, Ray GJ, DeWitt MA, et al. Enhancing homology-directed genome editing by  
348 catalytically active and inactive CRISPR-Cas9 using asymmetric donor DNA. *Nature biotechnology*  
349 2016;34(3):339-44, doi:10.1038/nbt.3481
- 350 15. Yao X, Zhang M, Wang X, et al. Tild-CRISPR Allows for Efficient and Precise Gene Knockin in  
351 Mouse and Human Cells. *Developmental cell* 2018;45(4):526-536.e5, doi:10.1016/j.devcel.2018.04.021
- 352 16. Miura H, Gurumurthy CB, Sato T, et al. CRISPR/Cas9-based generation of knockdown mice by  
353 intronic insertion of artificial microRNA using longer single-stranded DNA. *Scientific reports*  
354 2015;5(12799, doi:10.1038/srep12799
- 355 17. Riesenberger S, Kanis P, Macak D, et al. Efficient high-precision homology-directed repair-  
356 dependent genome editing by HDRobust. *Nature methods* 2023, doi:10.1038/s41592-023-01949-1
- 357 18. Wimberger S, Akrap N, Firth M, et al. Simultaneous inhibition of DNA-PK and Pol $\theta$  improves  
358 integration efficiency and precision of genome editing. *Nature communications* 2023;14(1):4761,  
359 doi:10.1038/s41467-023-40344-4
- 360 19. Chu VT, Weber T, Wefers B, et al. Increasing the efficiency of homology-directed repair for  
361 CRISPR-Cas9-induced precise gene editing in mammalian cells. *Nature biotechnology* 2015;33(5):543-8,  
362 doi:10.1038/nbt.3198
- 363 20. Maruyama T, Dougan SK, Truttmann MC, et al. Increasing the efficiency of precise genome  
364 editing with CRISPR-Cas9 by inhibition of nonhomologous end joining. *Nature biotechnology*  
365 2015;33(5):538-42, doi:10.1038/nbt.3190
- 366 21. Wilde JJ, Aida T, Del Rosario RCH, et al. Efficient embryonic homozygous gene conversion via  
367 RAD51-enhanced interhomolog repair. *Cell* 2021;184(12):3267-3280.e18, doi:10.1016/j.cell.2021.04.035
- 368 22. Song J, Yang D, Xu J, et al. RS-1 enhances CRISPR/Cas9- and TALEN-mediated knock-in efficiency.  
369 *Nature communications* 2016;7(10548, doi:10.1038/ncomms10548
- 370 23. Heyer WD, Ehmsen KT, Liu J. Regulation of homologous recombination in eukaryotes. *Annual*  
371 *review of genetics* 2010;44(113-39, doi:10.1146/annurev-genet-051710-150955

- 372 24. Hustedt N, Durocher D. The control of DNA repair by the cell cycle. *Nature cell biology*  
373 2016;19(1):1-9, doi:10.1038/ncb3452
- 374 25. Lin S, Staahl BT, Alla RK, et al. Enhanced homology-directed human genome engineering by  
375 controlled timing of CRISPR/Cas9 delivery. *eLife* 2014;3(e04766, doi:10.7554/eLife.04766
- 376 26. Eghbalsaid S, Kues WA. CRISPR/Cas9-mediated targeted knock-in of large constructs using  
377 nocodazole and RNase HII. *Scientific reports* 2023;13(1):2690, doi:10.1038/s41598-023-29789-1
- 378 27. Gu B, Posfai E, Rossant J. Efficient generation of targeted large insertions by microinjection into  
379 two-cell-stage mouse embryos. *Nature biotechnology* 2018;36(7):632-637, doi:10.1038/nbt.4166
- 380 28. Doyon Y, Choi VM, Xia DF, et al. Transient cold shock enhances zinc-finger nuclease-mediated  
381 gene disruption. *Nature methods* 2010;7(6):459-60, doi:10.1038/nmeth.1456
- 382 29. Miller JC, Tan S, Qiao G, et al. A TALE nuclease architecture for efficient genome editing. *Nature*  
383 *biotechnology* 2011;29(2):143-8, doi:10.1038/nbt.1755
- 384 30. Skarnes WC, Pellegrino E, McDonough JA. Improving homology-directed repair efficiency in  
385 human stem cells. *Methods (San Diego, Calif)* 2019;164-165(18-28, doi:10.1016/j.ymeth.2019.06.016
- 386 31. Guo Q, Mintier G, Ma-Edmonds M, et al. 'Cold shock' increases the frequency of homology  
387 directed repair gene editing in induced pluripotent stem cells. *Scientific reports* 2018;8(1):2080,  
388 doi:10.1038/s41598-018-20358-5
- 389 32. Maurissen TL, Woltjen K. Synergistic gene editing in human iPS cells via cell cycle and DNA repair  
390 modulation. *Nature communications* 2020;11(1):2876, doi:10.1038/s41467-020-16643-5
- 391 33. Remy S, Tesson L, Menoret S, et al. Efficient gene targeting by homology-directed repair in rat  
392 zygotes using TALE nucleases. *Genome research* 2014;24(8):1371-83, doi:10.1101/gr.171538.113
- 393 34. Taniguchi M, Sanbo M, Watanabe S, et al. Efficient production of Cre-mediated site-directed  
394 recombinants through the utilization of the puromycin resistance gene, *pac*: A transient gene-  
395 integration marker for ES cells. *Nucleic acids research* 1998;26(2):679-680, doi:10.1093/nar/26.2.679
- 396 35. Hitz C, Wurst W, Kühn R. Conditional brain-specific knockdown of MAPK using Cre/loxP  
397 regulated RNA interference. *Nucleic acids research* 2007;35(12):e90, doi:10.1093/nar/gkm475
- 398 36. Dolatshad H, Biggs D, Diaz R, et al. A versatile transgenic allele for mouse overexpression  
399 studies. *Mammalian genome : official journal of the International Mammalian Genome Society*  
400 2015;26(11-12):598-608, doi:10.1007/s00335-015-9602-y
- 401 37. Certo MT, Ryu BY, Annis JE, et al. Tracking genome engineering outcome at individual DNA  
402 breakpoints. *Nature methods* 2011;8(8):671-6, doi:10.1038/nmeth.1648
- 403 38. Lux CT, Pattabhi S, Berger M, et al. TALEN-Mediated Gene Editing of HBG in Human  
404 Hematopoietic Stem Cells Leads to Therapeutic Fetal Hemoglobin Induction. *Molecular therapy*  
405 *Methods & clinical development* 2019;12(175-183, doi:10.1016/j.omtm.2018.12.008

406

## 407 **Figure Legends**

408 **Figure 1:** GFP to BFP assay to assess HDR in human iPS cells. **A)** Schematic representation of the GFP to  
409 BFP system. A CAGGS promoter driven GFP cassette was integrated at the *AAVS1* locus. The position of  
410 the CRISPR-Cas9 target site is shown. If the resulting DSB is repaired by NHEJ and results in a indel that  
411 shifts the reading frame, the GFP will not be translated and the cells will not fluoresce. However, if the  
412 break is precisely corrected by HDR using an ssODN to introduce a Y66H mutation, the GFP sequence



413 will be converted into BFP, and cells will fluoresce blue. **B)** An example of an individual replicate of Flow  
414 cytometry analysis of iPS cells electroporated with CRISPR-Cas9 RNP with the ssODN and cultured for  
415 72h at 37°C or 24h at 30°C then 48°C at 37°C. Numbers shown inside plots indicate percentages of blue  
416 or non-fluorescing cells. **C)** Histogram showing the percentage of GFP negative (GFP-) or BFP positive  
417 (BFP+) cells for the three technical replicates performed. **D)** Histogram showing the ratio of HDR/NHEJ  
418 for the three technical replicates performed.

419 **Figure 2:** Traffic light reporter to assess HDR in mouse ES cells. **A.** Schematic representation of the TLR  
420 system. A CAGGS promoter driven mRFP1 cassette harbouring an disruptive 27 bp deletion, followed by  
421 an out-of-frame P2A-GFP cassette was integrated at the *Gt(ROSA26)Sor* locus. The position of the  
422 CRISPR-Cas9 target site is shown. If the resulting DSB is repaired by NHEJ and results in an indel that  
423 shifts the reading frame, the GFP may be brought into frame and the cells will fluoresce green. However,  
424 if the break is precisely corrected by HDR using an ssODN to repair the 27 bp deletion, the mRFP1  
425 sequence will be restored and the cells will fluoresce red. **B)** An example of an individual replicate of  
426 Flow cytometry analysis of ES cells electroporated with CRISPR-Cas9 RNP with the ssODN and cultured  
427 for 72h at 37°C or 24h at 30°C then 48°C at 37°C. Numbers shown inside plots indicate percentages of  
428 red or green cells. **C)** Histogram showing the percentage of GFP or mRFP1 expressing cells for the three  
429 technical replicates performed. **D)** Histogram showing the ratio of HDR/NHEJ for the three technical  
430 replicates performed.

431 **Figure 3:** The effects of cold shock on mouse embryos. **A)** Schematic design of the knock-in experiment  
432 in mouse embryos. One-cell embryos were electroporated using CRISPR-Cas9 RNP and ssODN designed  
433 to target different loci. Embryos were cultured at 37°C for the control group or at 30°C for 6h followed  
434 by 37°C for the cold shock group. At blastocyst stage, embryos were individually harvested and  
435 genotyped. **B)** Overall HDR efficiency for the three different genes. **C)** Knock-in efficiency showing the  
436 results of the 5 independent sessions, comparing activity at the three tested genes, illustrated as a box

437 plot (25%-75% percentile, with the whiskers extending to the minimum and maximum values. **D)** Overall  
438 editing efficiency (indel or knock-in) for the 5 independent sessions performed, as a box plot as C). **E)**  
439 Two litters of mice generated from the in vivo albino mutation correction experiment performed under  
440 control conditions (37°C) or with cold shock (30°C).

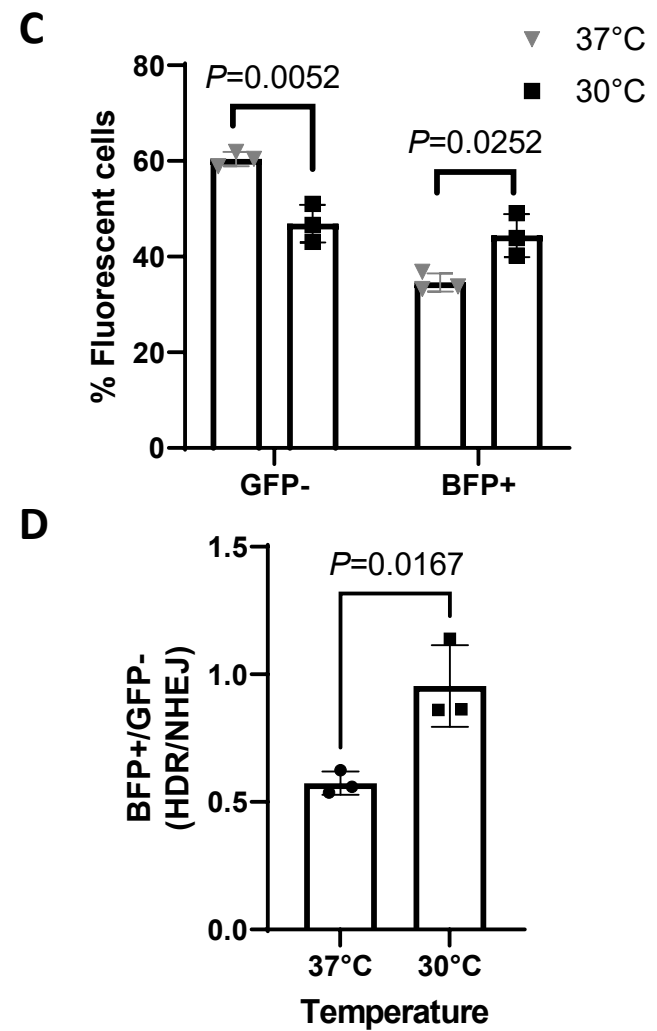
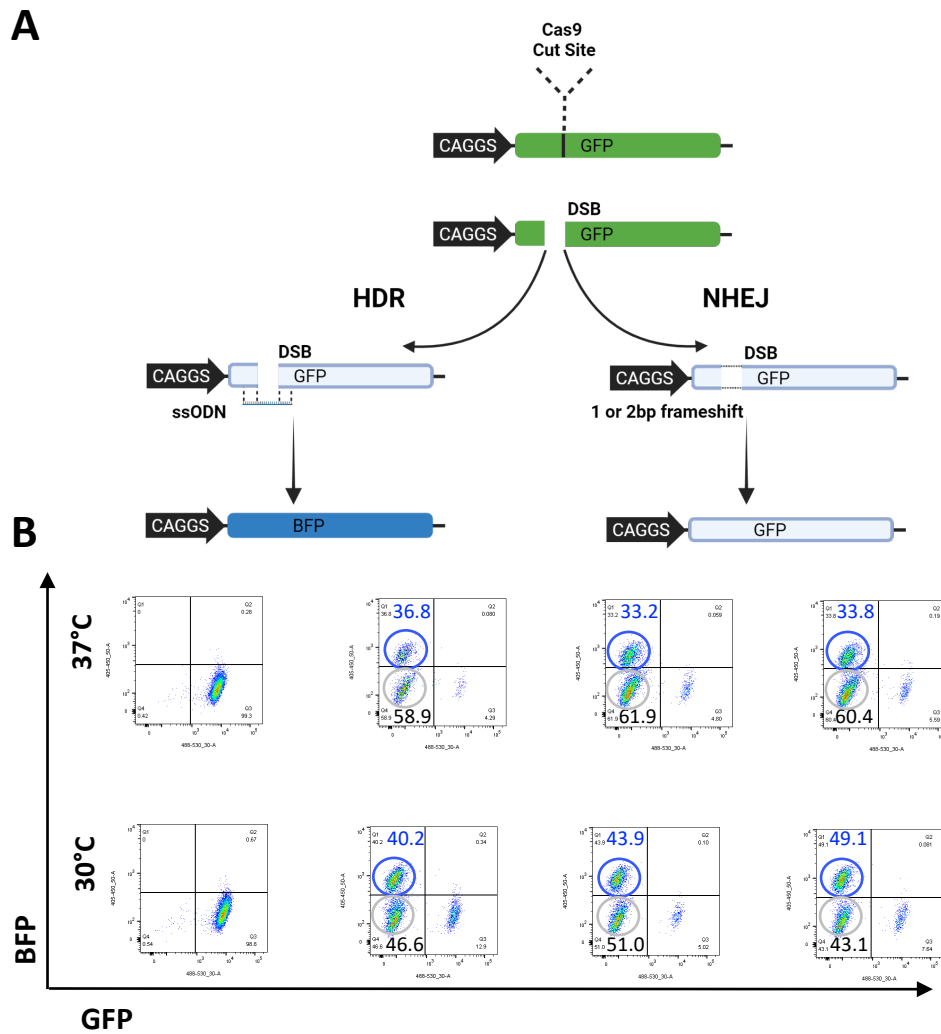


Figure 1

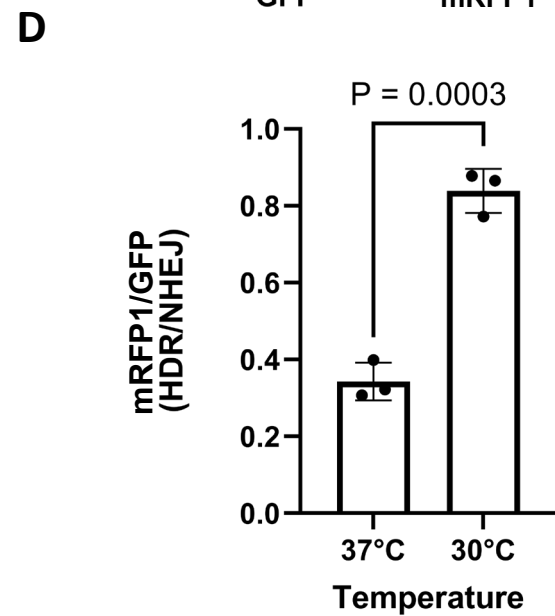
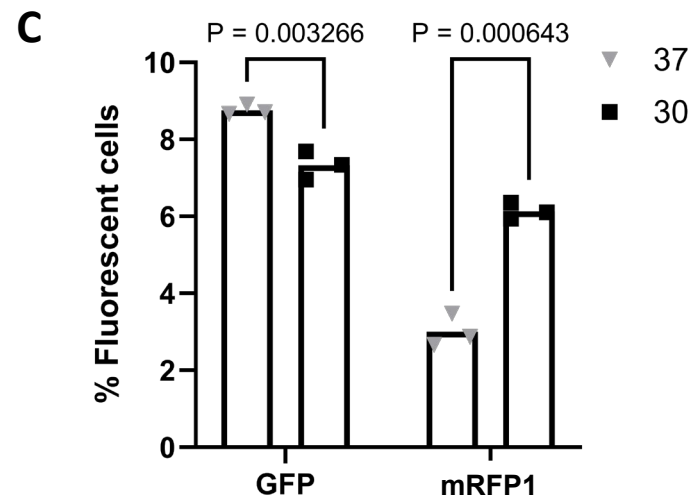
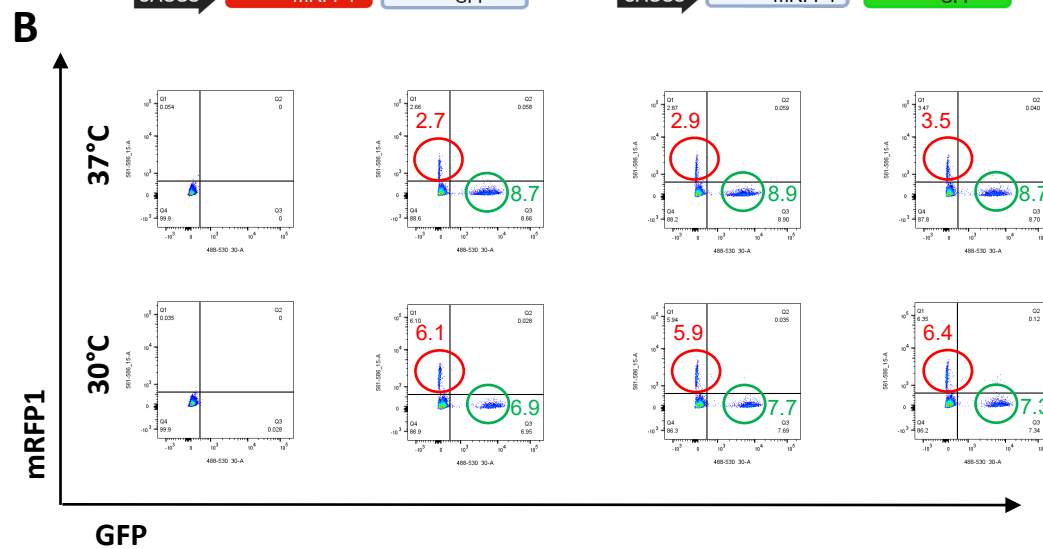
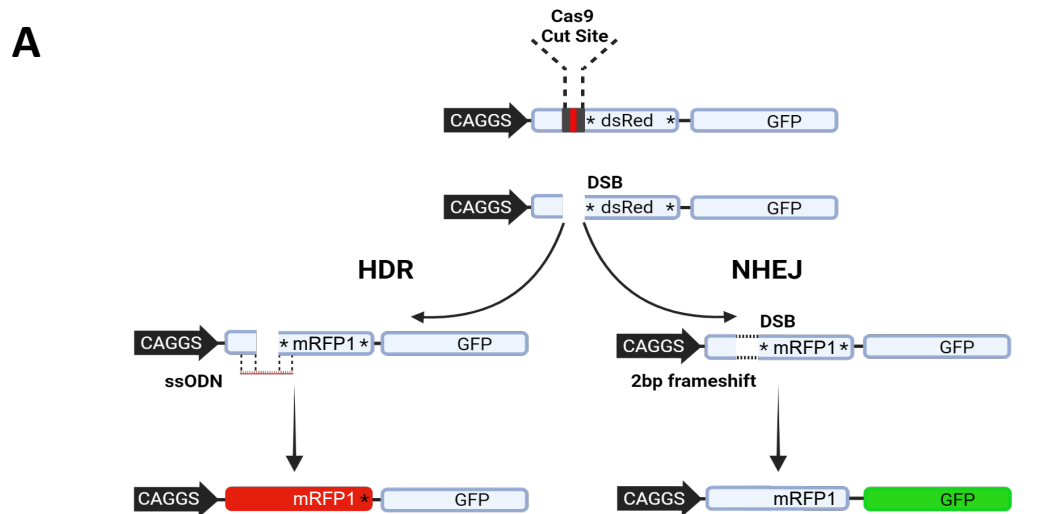


Figure 2

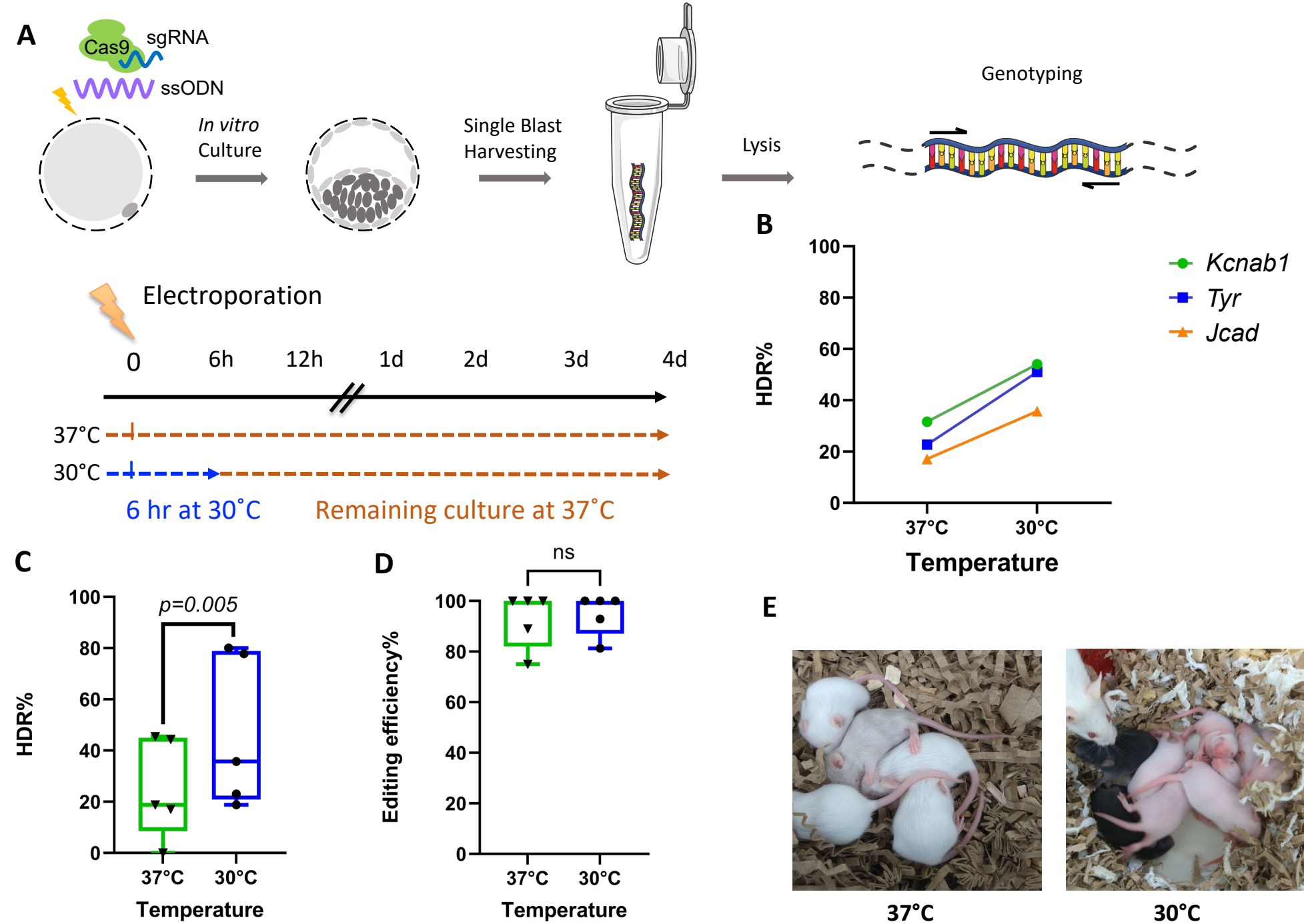
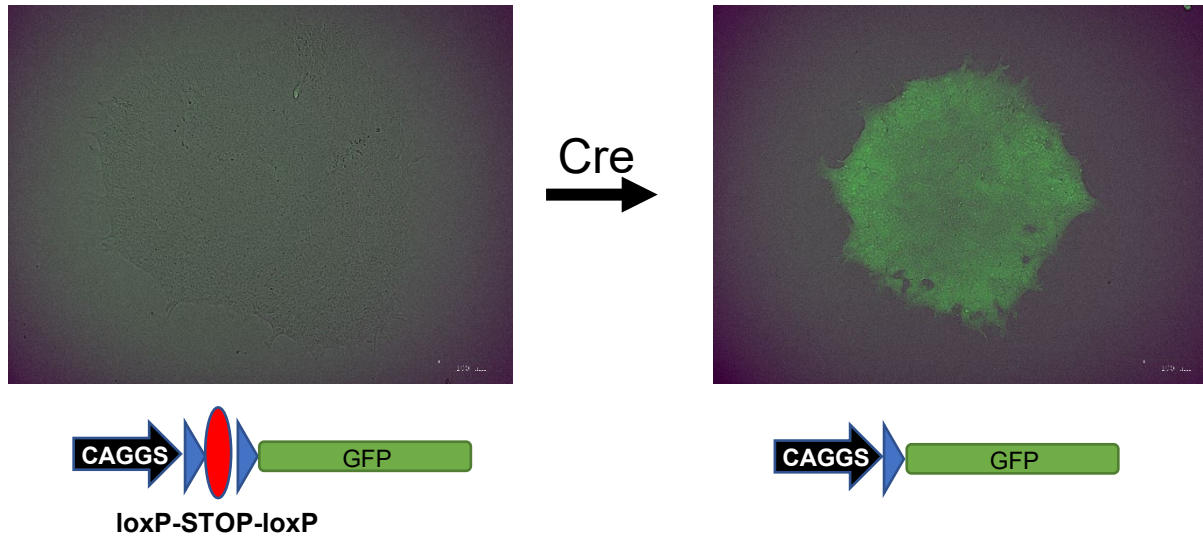
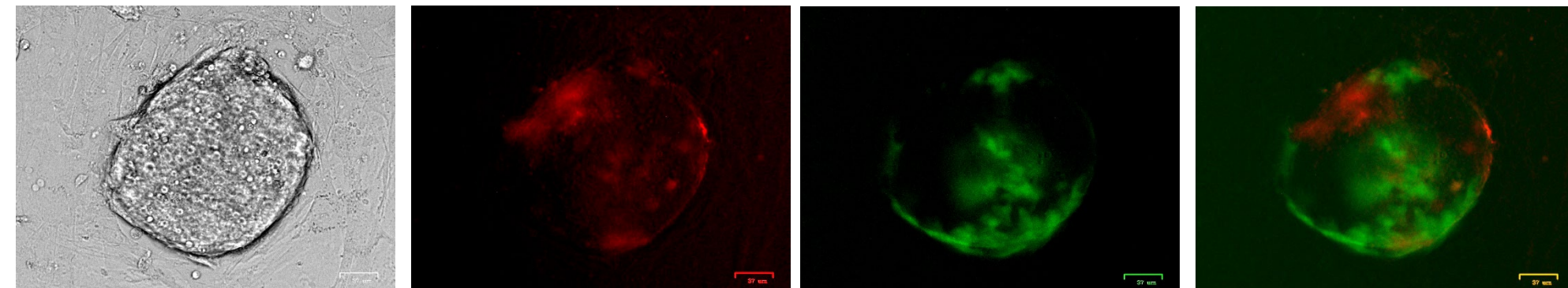
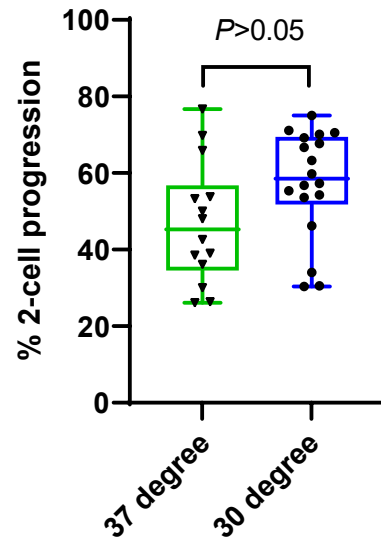
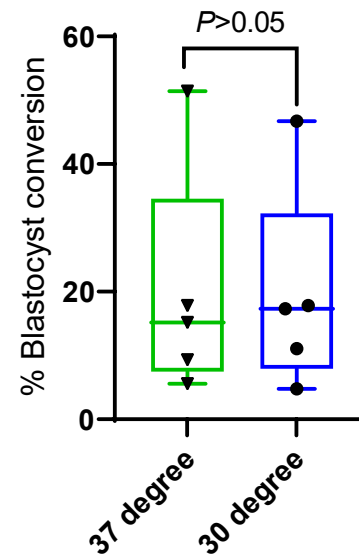


Figure 3

**A****B**

**Supplementary Figure 1: A)** Human iPS cells with a CAGGS promoter–loxP-STOP-loxP-GFP cassette inserted at the *AAVS1* locus. Following Cre recombinase transfection, the excision of the STOP signal activates GFP expression leading to homogenous expression within the iPS cells. **B)** Imaging of a mouse ES cell colony harbouring the Traffic Light Reporter inserted at the *Gt(ROSA26)Sor* locus. The cells have been electroporated with an sgRNA targeting the inactive mRFP1 gene with an ssDNA to restore its function. The GFP expression is indicative of NHEJ repair, with a frame-shift of +2 due to an indel restoring the reading frame of the GFP gene, whereas the mRFP1 expression is indicative of HDR repair, with the mRFP1 corrected by successful recombination with the repair ssODN.

**A****B**

**Supplementary Figure 2** – Effects of subjecting 1-cell zygotes to 6-8 hours of 30°C cold-shock on A) mouse 2-cell development and B) blastocyst development

Target Locus	Rep. colour	Protospacer 5'-3'	Genomic coordinates	Forward Genotyping Primer	Reverse Genotyping Primer
<i>Jcad</i>	Orange	GCATGCCTTCAGGCTGACAT	Chr7: 87,073,979-87,142,720 (-)	CTGGCAAAGTCCTGCAGTTG	ACATTGGTCCCTATGGTGGT
<i>Kcnab1</i>	Green	CTCTACATGGCATCATTGG	Chr3: 64,856,617-65,285,644 (+)	CCCAGTGTCTGAGGGTAGGA	CACCCACGTTTCATTCCAGGA
<i>Tyr</i>	Blue	GGGTGGATGACCTTGAGTCC	Chr18: 4,634,878-4,682,869 (+)	AGGAGAAAATGTTCTTGGCTGTTTTGT	CTTGTTCCCACAATAACAAGAAAAGTCTGT
<i>TLR</i>	Grey	GGCCACGAGTTCGAGATCTA	NA	NA	NA
<i>GFP</i>	Grey	CTCGTGACCACCCTGACCTA	NA	NA	NA

**Supplementary Table 1:** Targets for CRISPR/Cas9 mutagenesis together with their genomic coordinates and the primer sequences used for genotyping.



Target Locus	Rep. colour	Template length (nt)	Template sequence	Restriction site
<i>Jcad</i>	Orange	139	CAAAGGTTTAGTCCGTTATCATTATGGTAGGAAGCATGCCTTCAGGCTGAAGCTTATAACTTCGTATAATGT ATGCTATACGAAGTTATCATTGGAGCAGTAGCTGAAAACACATCCTGATCCTTAGGTGGACAGACA	HindIII
<i>Kcnab1</i>	Green	200	AGGTTGCTGAACGGCTGATGACAATTGCCTACGAAAGTGGAGTTAATCTCTTCGACACAGCTGAGGTCTtT GCTGCTGGGAAGTAAGTCAGAACAAGTTTTTAGCTCTCACATGGCATCATTGGTaaagcttGGAAGCAAGAGG GTGTGCTCAAACATTGCTGTGGCATTGGCAAGGAGGGACTGCTCTTCTGTACATAT	HindIII
<i>Tyr</i>	Blue	139	CCAGGATATCCTTCTGTCCAGTGCACCATCTGGACCTCAGTTCCCCTTCAAAGGGGTGACGATCGTGAAA GCTGGCCCTCTGTGTTTTATAATAGGACCTGCCAGTGCTCAGGCAACTTCATGGGTTTCAACTG	PvuI
<i>TLR mRFP1</i>	Grey	150	AAGGTGCGCATGGAGGGCTCCGTGAACGGCCACGAGTTCGAAATTGAGGGCGAGGGCGAGGGCCGCCCC TACGAGGGCACCCAGACCGCCAAGCTGAAGGTGACCAAGGGCGCCCCCTGCCCTTCGCCTGGGACATCC TGTCCTCAG	NA
<i>GFP-to-BFP</i>	Grey	138	CCTGAAGTTCATCTGCACCACCGGAAGCTGCCCCGTGCCCTGGCCCCACCTCGTGACCACCCTGAGCCACG GCGTGAGTGTCTCAGCCGCTACCCCGACCACATGAAGCAGCAGACTTCTCAAGTCCGCCATGCC	NA

**Supplementary Table 2:** ssODN repair templates and the diagnostic restriction enzyme site used for detection

Gene ID	Condition	Inclusion of HDR template	No. harvested	No. used	No. survived	No. 2-cell	% 2-cell	No. blastocysts <sup>h</sup>	% Blast/survived	% Blast/2-cell	HDR	Mut	Total analysed
<i>Jcad</i>	37°C	Yes	70	70	63	44	70%	36	57	82	6	31	35
<i>Jcad</i>	30°C	Yes	60	60	56	42	75%	28	50	67	10	26	28
<i>Kcnab1</i>	37°C	Yes	60	60	54	23	43%	9	17	39	4	9	9
<i>Kcnab1</i>	30°C	Yes	60	60	54	36	67%	9	17	25	8	9	9
<i>Kcnab1</i>	37°C	Yes	90	90	90	48	53%	16	18	33	3	12	16
<i>Kcnab1</i>	30°C	Yes	90	90	90	64	71%	16	18	25	3	13	16
<i>Tyr</i>	37°C	Yes	105	105	105	41	39%	16	15	39	0	16	16
<i>Tyr</i>	30°C	Yes	75	75	75	43	57%	13	17	30	3	13	13
<i>Tyr</i>	37°C	Yes	130	130	125	33	26%	12	10	36	5	12	12
<i>Tyr</i>	30°C	Yes	130	130	125	38	30%	12	10	32	8	12	12

**Supplementary Table 3:** Production and genotyping summary data for the generation of blastocysts using CRISPR/Cas9 reagents and ssODN delivered by electroporation under normal (37°C) or cold-shock (30°C) conditions.

Gene ID	Condition	Inclusion of HDR template	No. harvested	No. used	No. survived	No. 2-cell	% 2-cell	No. of transfers*	Pups born %	White	Chimera	Black
									No. pups/ no.transferred(%)			
<i>Tyr</i>	37°C	Yes	239	239	235	30	13%	3	7/70 (10%)	6	1	0
<i>Tyr</i>	30°C	Yes	321	321	291	99	34%	4	16/138(11.59%)	14	0	2

**Supplementary Table 4:** Production and genotyping summary data for the generation of live pups using CRISPR/Cas9 reagents and ssODN delivered by electroporation under normal (37°C) or cold-shock (30°C) conditions.